Electronic Functionality of Nanocomposites

Pandiyan Murugaraj and David Mainwaring
School of Applied Sciences, College of Science, Engineering and Health, RMIT University
Australia

1. Introduction

Functional polymer nanocomposites have the potential to improve the performance of both active and passive components in advanced electrical devices. Electrically conducting nanocomposites are a growing research focus for such applications in light weight flexible electronics particularly in strategic infrastructure. Such materials also open up a broad range of fabrication techniques which can be easily used in mass manufacturing via imprinting to yield low-cost devices. Here, the mechanisms of electron transport in these polymer nanocomposites are addressed in terms of modifications to existing theories of variable range electron hopping and fluctuation induced tunnelling originally applied to heavily doped semiconductors and granular metal composites. The fabrication and behaviour of two types of nanocomposites that involve dispersed carbon nanoparticles in a polymide medium and carbon nanocluser composites formed by ion irradiation of polyimide are compared through their conduction mechanisms and sensing performance.

2. Electron transport phenomena

2.1 Electron transport mechanisms

Electron transport phenomena in 3-D composite structures remains an area of significant research interest. Earlier work was predominately carried out on granular materials particularly discontinuous metal thin films on dielectric substrates. With increasing interest in electrically functional polymer composites, the existing theoretical approaches are being re-addressed to accommodate transport behaviour these materials. Mott (1969) originally addressed disordered systems where the electronic states are localised near the Fermi level and the electric conduction does not follow classic processes of diffusion but rather a variable range hopping (VRH) mechanism. According to Mott's theory for a 3D system, the temperature dependent conductivity (σ) is governed by the expression:

$$\sigma = \sigma_o \ \exp \{-(T_o/T)^{1/4}\} \tag{1}$$

where σ_o and T_o are constants and T the absolute temperature. Here, the density of energy states was considered constant while the interaction between these charge states was not considered (Mott, 1969, Efros & Shklovskii, 1975). Subsequent application of Mott's theory to various systems such as amorphous semiconductors, heavily doped semiconductors, cermets and polymer composites have shown a clear deviation from the $T^{1/4}$ temperature dependent conductivity, even though these systems form spatially distributed localised

energy states arising from defects and impurities as envisaged in Mott's original expression (Sheng & Klafter, 1983).

Even though the hopping mechanism is considered to be dominant in electron transport in such disordered materials and conducting composites, the temperature dependence of conductivity is now considered to follow a more generalised Arrhenius relationship $\sigma = \sigma_o exp\{-(T_o/T)^{1/\gamma}\}$ having the exponent γ ranging from 1 to 4 thus indicating a more complex behaviour involving more than one type of thermally activated conduction mechanism (Sheng & Klafter, 1983, Adkins, 1987). These deviations may arise from the two assumptions above imposed in the Mott's theory as well as from inhomogenous spatial distributions of charge states, particles sizes and morphologies (Devenyi et al., 1972, Neugebauer & Webb, 1962). Additionally, systems in which the electrons are delocalised over large atomic distances such as structured carbon black composites, large metal island films and high aspect ratio structures, have electron transport dominated by large conducting segments (aggregates) rather than by hopping between well localised states (Sheng et al., 1978).

Using a similar approach to Mott, Efros & Shklovskii (Efros, 1976, Efros & Shklovskii, 1975) (ES) introduced a Coulomb gap into the description of the density of states near the Fermi level to account for the electron-electron interactions which diminish the density of states in this region. It was assumed here that the quantum localisation length was much smaller than the distance between the centres of the charged particles in these granular systems resulting in negligible overlap of the wavefunctions. According to Efros' formulation, the Coulomb gap (Δ) plays an important role in the low temperature conductivity where the energy interval responsible for hopping (ε_M) is comparable or greater than the Coulomb gap ($\varepsilon_M < \Delta$) in Mott's expression:

$$\varepsilon_M = T^{3/4} / (\alpha^3 g_o^{1/4}) \qquad (2)$$

here α is the localisation length and g_o is the density of states at the Fermi level. Efros and Shklovski argued that the Coulomb interaction causes the appearance of a gap within the density of states which when incorporated into Mott's theory leads to a $T^{1/2}$ dependence. Thus according to this modified theory, $T^{1/2}$ behaviour should be seen at low temperatures and $T^{1/4}$ behaviour must be observed at higher temperatures, with a transition occurring at T_{ES}. Chui et al. (1981) applied this theory to high resistivity granular samples and found that its temperature dependence was not entirely consistent and concluded that the low density of states in these systems caused such a discrepancy. Entin-Wohlman et al. (1983) subsequently analysed a similar system theoretically accounting for the roles of the metal-insulator transition as well as the diverging dielectric permittivity near this transition and found it qualitatively agreed with the ES theory. Shekhar et al. (2006a) studying the temperature dependent electrical conductivity of an iron carbide/polymer composite system identified an anomalous Mott variable range hopping conduction mechanism having a T_{ES} crossover from one type of ES-VRH to another type with changing composite compositions.

Klafter & Sheng (1984) (KS) also proposed an advance to Mott's theory to account for the $T^{1/2}$ relationship observed with granular materials in terms of a "charging or tunnelling" modification which took into account electron tunnelling from one neutral grain to another thus creating two oppositely charged species. As a consequence of the small but definite capacitance this induces, the overall process involves a charging energy representing the

minimum positive energy required for electron transfer between the initial neutral grains which becomes the source of the Coulomb gap for the excitation of charge carriers in each grain. Additionally, this approach used a modified density of states which then demonstrated the $T^{1/2}$ behaviour as an interpolation across the whole temperature range of these Mott type systems. Subsequently McAlister et al. (1984) applied the KS theory to Au/SiO$_2$ systems over the temperature range 4 – 300K and found it represented the behaviour more exactly than the ES approach.

More recently, Mainwaring et al. (2008) studied the temperature dependent electron transport properties of a carbon nanoparticle polymer composite thin film exhibiting semiconducting behaviour over the temperature range 20 – 450K in terms of Mott's 3-D VRH theory, and found that the behaviour can be explained well by adoption of the KS modification to Mott's approach to electron conduction. This approach took account of the statistical distribution of granular particles which leads to a distribution of gaps and charging energies as well as random potential energies arising from thermally induced voltage fluctuations, as Adkins (1989) predicted for a simple activation type of conduction given by:

$$\sigma \propto \exp(-2\alpha s - W/kT) \tag{3}$$

where α is the exponent of electron wavefunctions in the dielectric medium, s the separation between the grains, and W the charging energy. While the predicted activation energies were of the correct order of magnitude, the temperature exponent (x) varied between 0.3<x<1.0 for Adkins' system:

$$\sigma \propto \exp(T_o/T)^x \tag{4}$$

Accordingly, Adkins investigated electron – electron correlation and the presence of a Coulomb gap to further modify the theory and found it closely predicted the temperature dependence of metal granular systems, although the optimum hopping distances (R_{opt}) and the barrier heights (<kT) obtained from these fits were unrealistically small to accurately consider the mechanism as totally electron hopping.

2.2 Polymer conductors

Conductive polymer composites initially consisted of conducting particles at sufficient concentrations to form percolating transport networks within the insulating medium. Subsequently an increasing interest has grown in intrinsically conductive polymers such as the doped conjugated systems which now provide both metallic and semiconductive behaviour. In organic semiconducting materials such as most conjugated polymers and many amorphous molecular materials conduction is governed and limited by thermally activated hopping mechanisms. Here highly ordered short chain conjugated oligomers allow very high mobilities to be achieved (Garnier, 1998, Hatchett & Josowicz, 2008, Kaiser, 2001). With electron movement along the chains, the electrical conductivity is quasi one dimensional and hence is highly anisotropic depending on the orientation of the polymer chains during polymerization. The conductivity is further influenced by morphological inhomogeneity (Kryszweski & Jeszka, 2003) within the system.

Fluctuation induced tunneling is the dominant mechanism in these polymer structures where extended metallic-like regions separated by narrow imperfect potential barriers prevail as expressed in:

$$\rho(T) = \phi_1\,\rho_m\,\exp\{-(T_m/T)\} \;+ \phi_f\rho_t\,\exp\{T_t/(T+T_s)\} \tag{5}$$

where ϕ_1 and ϕ_f are weighing factors while T_m, T_t and T_s characteristic temperatures and ρ_m, ρ_t pre-exponential factors of the relative transport processes (Kaiser, 2001). Here, electrical conductivity is modelled in terms of an equivalent circuit consisting of resistors connected in series or parallel depending on the extent of polymer crosslinking. A second mechanism operates when small crystalline regions are dispersed within amorphous regions, electron transport is then represented by the charging energy limited tunnelling VRH as given by Kaiser (2001):

$$\rho(T) = \phi_1\,\rho_m\,\exp\{-(T_m/T)\} \;+ f_f\rho_t\,\exp\{(T_o/T)^\gamma\} \tag{6}$$

where T_o is a constant dependent on the wavefunction decay and the density of states at the Fermi level and the exponent γ depends on the dimensionality of charge transport. Electrical conductivity is also influenced by chain length as well as defect concentration. The conductivity can then be tuned by chemical manipulation of the polymer backbone, any dopants, as well as by blending with other polymers.

In the metallic-like polymer behaviour, the earlier expressions above predict unrealistic low resistivities below 100K, however in real systems considerable electron scattering exists which results in a residual finite resistance. Kryszewski & Jeszka (2003) modified Kaiser's expression to include this as an additional resistance term (ρ_o).

Electron transport in particulate polymer composite thin films normally involves activated transport between conducting particles separated by potential barriers or dielectric medium (Devenyi et al., 1972, McAlister et al., 1984). At higher particle concentrations, percolating networks form which provide simple metallic-like conduction at ambient temperatures and exhibit anomalous (abrupt) decreases in conductance at elevated temperatures which may arise from structural changes occurring in the polymer medium such as glass transition, crystallization and melting. This unique property of polymer composites has been exploited in current limiting and switching devices as well as self regulating heaters (Shermann et al., 1983, Fournier et al., 1997). Particle concentrations just below the percolation threshold result in isolated particles or particle clusters dominating electron transport. This non-percolating dielectric regime involves thermally activated tunnelling of charge carriers between nearest neighbour particles at sufficiently close proximity to enable overlap of the electron wave functions of each particle similar to the granular films discussed above. At even greater particle separations variable range hopping now provides conductivity through an optimal network of electron hopping sites (Klafter & Sheng, 1984).

2.3 Nanoparticle – polymer composites

Carbon nanoparticle composite films can be produced by either physical blending techniques followed by film casting where the dispersion may be formed either in the molten state or in solution (Hanemann & Szabo, 2010). Film casting techniques are dominated by either spin coating on to substrates or slip casting to produce free standing films. As an alternative, nanoparticle dispersions in polyimide (PI) monomer solutions followed by film formation and thermal curing can be employed to produce highly homogeneous composite thin films which may be either supported or free standing (van Zyl et al., 2002, Mora-Huertas et al., 2004).
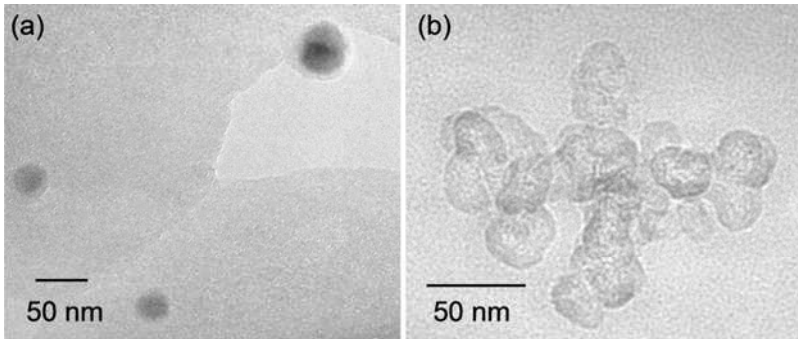
Fig. 1. Electron micrograph (HRTEM) of microtomed sections of C nanoparticle-PI composite film: (a) single particles; (b) aggregate.

Carbon nanoparticle – polyimide (C-PI) thin films can be prepared by the in-situ polymerization technique for a wide range of molecular compositions which yield either single nanoparticle and nanocluser dispersions as shown in Fig. 1 for the polyimide benzophenone tetracarboxylic dianhydride and 4,4′-oxybisbenzenamine (BTDA-ODA). The temperature dependence of resistance of these films over a wide temperature range from 20K to 450K is shown in Fig. 2(a-c). Fig. 2(a) shows the electrical resistance as a function of $1/T^{1/4}$ for a 5 vol.% C-PI film, where the resistance decreased monotonically typical of semiconducting behaviour following Mott's 3-D VRH mechanism according to expression (1). Here, electron transport can be seen to follow the $1/T^{1/4}$ relation well only over the limited temperature range 28 to 63K. Above this, the deviation from $1/T^{1/4}$ increases and forms a transition to the $1/T^{1/2}$ behaviour shown in Fig. 2(b) across the temperature range 53 to 230K. Above this temperature range (Fig. 2(c)), a further deviation produces simple linear thermal activation with a $1/T$ process up to 343K. Above this maximum temperature, a further deviation indicates the on-set of contributions from metallic-like scattering within the nanoparticle clusters.

According to Mott's original treatment of 3-D VRH in amorphous semiconductors, resistance is given by:

$$R = \frac{kT}{e^2 r \omega_0} \exp\left(\frac{W}{kT}\right) \exp\left(\frac{2r}{\xi}\right) \qquad (7)$$

here r is the spacing between the localised energy levels, ω_0 the attempt frequency given by the typical phonon frequency, k the Boltzman constant, W the activation energy, and ξ the Anderson's localization length. In equation 7, the overlap function $e^{2r/\xi}$ favours short hops while the activation term $e^{(W/kT)}$ favours long hop distances. Electron transport then results from an optimized competition between short and long hops as observed in conventional doped semiconductors at low temperatures (Mott & Davis, 1979). Fig. 2 indicates that the $1/T^{1/2}$ behaviour observed across the intermediate temperature range arises from a combination of low temperature $1/T^{1/4}$ behaviour and simple Arrhenius activated conductivity at higher temperatures (Mainwaring et al 2008). Overlaps in these temperature intervals provide gradual transitions in behaviour, such that the data over the extended range conforms to the model predicted by Klafter & Sheng (1985).
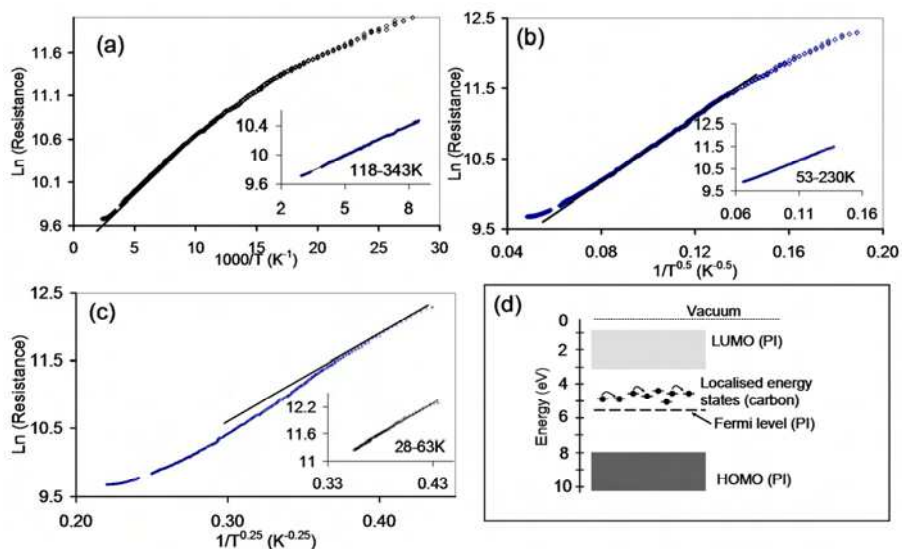
Fig. 2. Temperature dependent electrical resistance of 5 vol% C nanoparticle–PI composite thin film as: (a) $1/T^{0.25}$; (b) $1/T^{0.50}$ and (c) $1/T$. Insets show ranges that conform to T exponents, and (d) schematic representation of the proposed energy level diagram.

These temperature dependencies illustrate that carbon – polyimide nanocomposites have electrical responses very similar to granular metals such as Au – SiO_2 (McAlister et al., 1984) where metal islands form spatially distributed localized electronic states located between the valance band and the conduction band of the oxide dielectric medium. Thermally activated hopping of charge carriers between these localized states give rise to the observed electrical conductivity, which are observed in both polymer systems (Shekar et al., 2006a).

The corresponding energy diagram (Fig. 2(d)) illustrates this dispersion of carbon nanoparticles in the polyimide matrix forming localized electronic states between the highest occupied molecular orbital (HOMO) and lowest unoccupied molecular orbital (LUMO) of the polymer medium. The BTDA-ODA polyimide shown has a band gap of about 7 eV and an ionization potential of 8.97 eV similar to PMDA-ODA (Kafafi et al., 1990), while the work function of the graphitic nanoparticles is about 4.6 eV (Suzuki et al., 2001). Carbon nanoparticles can then be approximated as spatially distributed localized electronic states 2.67 eV below that LUMO of the undoped polyimide, which is ~0.9 eV above the Fermi level.

Differential thermal expansion of polymer nanocomposite thin films significantly influences the total electrical conductivity (σ_t (T)) particularly at higher temperatures. It can be considered to have the following contributions:

$$\sigma_T (T) = \sigma (T) + \Delta_1\sigma (T) + \Delta_2\sigma (T) + \Delta_3\sigma (T) \tag{8}$$

where $\sigma(T)$ arises from thermal activation of charge carriers which governs both variable range hopping and thermally induced fluctuation induced tunnelling mechanisms and as such is a positive quantity for semiconductor systems. The thermal expansion effect $\Delta_1\sigma$ (T) arises from the differences in the coefficients of thermal expansion between the conducting

nanoparticles (2×10^{-6}m/°C) and polymer (150×10^{-6} m/°C). Similarly $\Delta_2\sigma$ (T) arises from carrier scattering within the regions of pseudometallic behaviour which is negative and dominates at room temperature and above. Temperature dependent structural properties of the polymer matrix including the degree of crystallinity, glass transition temperature and melting behaviour gives rise to a further contribution $\Delta_3\sigma$ (T). Overall these contributions decrease the effective volume fraction of the conducting regions, decreasing the conductivity across the whole temperature range (Mora-Huertas et al., 2004). Modelling has shown that differential thermal expansion can impose compressive and tensile stresses between well adhered composite particles and the surrounding polymer medium (Klemens et al., 1986). By analogy to other systems (Aneli et al., 1999a), such stresses can alter the local electronic structure of localised energy states through band bending for example and thereby influence electron transport parameters such as barrier height and mobility. When particle adhesion is poor, Sherman et al., (1983) showed that thermal expansion results in delamination causing anomalous changes in conduction with temperature. Particle size within composites also affects conduction such that smaller particles with very small interfacial areas reduce the influence of differential thermal expansion compared to larger particles at similar volume fractions (Sheker et al., 2006b, Zhu et al., 2007) since they effectively provide a more homogeneous system.

2.4 Nanocluster – polymer composites

Various techniques have explored the fabrication of nanocluster polymer composite films. Nanoclusters may be considered as structures that have their interface predominately consisting of surface atoms such that interfacial interactions occur virtually between all atoms, as reviewed by Jena et al. (2001). Such fabrication techniques include:

- physical deposition such as co-deposition of polymer films together with metallic or carbon clusters (Grytsenko & Schrader, 2005, Wei & Eilers, 2008),
- electrochemical deposition forming metallic nanoclusters within conducting polymer matrices combining electropolymerization and controlled electrodeposition (Trung et al., 2005),
- sol gel processing forming metallic or metal oxide nanoclusters within polymers with and without templates (Groehn et al., 2001, Nandi et al., 1990, O'Connor et al. 1997, Di Gianni et al., 2007), and
- ion implantation at low energies (< 100 keV) with metal ions in the fluence range 10^{15} to 10^{17} ions cm^{-2} (Di Girolamo et al., 2010).

High energy ion beam irradiation also produces carbon nanoclusters in polymer films such as polyimide allowing the homogeneous formation of carbonised inclusions within tracks in the polymeric medium (Hioki et al., 1983, Davenas et al., 1988, Murugaraj et al., 2009a). It has also been shown that these clusters always occur when aromatic heterocyclic moieties are present in the original polymeric film (Davenas et al., 1988). High-energy ion penetration of the polymer results in bond cleavage, chain scission and the formation of free radicals along its path as energy dissipates to the surrounding matrix, leaving carbon enriched regions and stable free radicals in the region surrounding the ion track (Murugaraj et al., 2009a, 2010b). Modeling of the ion trajectory and the penetration depth using SRIM numerical simulation (Ziegler et al., 2008) shows that ion tracks critically depend on the irradiation energy parameters as well as the physical and chemical characteristics of the polymer. In general irradiation levels below fluences of 10^{13} ions cm^{-2} produce well

separated ion tracks (Fink et al., 1995, Fragala et al., 1998), while fluences above this results in multiple overlapping tracks. Within both the single and overlapping tracks, carbon enriched graphitic clusters become a source of electron transport. Ion induced electrical conductivity can be produced by two differing mechanisms. The first results from the formation of graphitic tracks at sufficient density to yield graphitic-like layers such as those related to the glassy carbon structures (Feurer et al., 1993, De Bonis et al., 1999). The second represents a progression of chemical modification resulting from thermal transformations yielding a gradual modification of the band structure from semiconducting behaviour at low fluences to metallic conduction at high fluences (De Bonis et al., 1999, Costantini et al., 2002). When the ion beam parameters are controlled to prevent bulk carbonisation, it has been shown that irradiation produces randomly distributed graphitic clusters (Fink et al., 1996, Murugaraj et al., 2009a, 2010b).
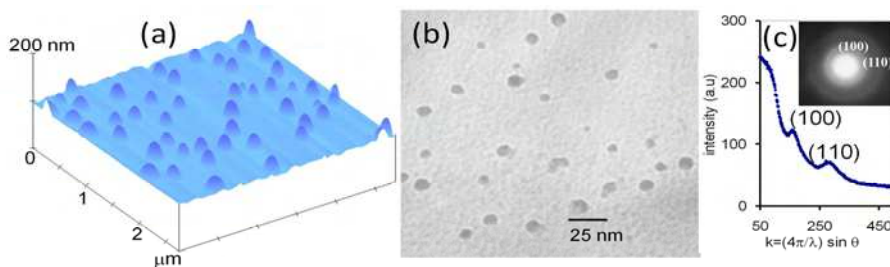
Fig. 3. Microstructure of the C nanocluster-PI composite films (4.5 MeV Cu^{3+} at fluences $<10^{11}$ ions cm^{-2}: (a) AFM tapping mode; (b) HRTEM of planar section and (c) SAED pattern of the ion tracks.

Originally, irradiated polyimide films at low fluences were considered as   low-loss insulators (Salvetat et al., 1997) which showed a small increase in dielectric constant (ε) attributable to electrical inhomogeneities originating within the ion tracks themselves rather than structural reorganization in irradiated regions, although recent work has shown that there are significant changes in the dielectric permittivity on ion irradiation (Murugaraj et al. 2009). The 3-D conductivity in the track overlapping region is recognized as a result of the carbon clusters producing spatially distributed charges within the polymer together with specific localized energy states in their electronic structure. Charge transport then results from fluctuation induced tunneling (FIT) at low temperatures (Phillips et al. 1993, Davenas et al., 1988, Salvetat et al., 1997) and hopping via thermal activation process at elevated temperatures (Murugaraj et al., 2009a).

AFM imaging of ion beam irradiated   polymer films in both the single track and the multiple overlapping track regime shows the microstructural changes of the surface resulting from track formation. Fig. 3(a) clearly illustrates surface hillocks associated with non-overlapping tracks comprising carbon nanoclusters ejected during escape of volatile gases (O_2, N_2, H_2 and $C-H_x$) produced within the polyimide medium during the interaction of high energy ions with the molecular chains (Fink et al., 1996, Toulemonde et al., 2004, Murugaraj et al., 2010). High resolution electron microscopy of the planar section of this irradiated film (Fig. 3(b)) reveals 15-25 nm diameter circular cross sections of these carbon channels (Murugaraj et al., 2010). Adla et al. (2003) used chemical staining techniques to delineate such tracks in polymers when they are microtomed and observed by TEM.

Selected area electron diffraction has shown preferential orientation of the carbon nanostructures formed within these channels by the appearance of only (100) and (110) rings of graphitic-like structures when observed in planar section (Fig. 3(c)). The absence of the major diffraction peak (002) due to the graphitic basal planes confirms the orientation of these graphitic nanoclusters parallel to the irradiation direction (ion beam path).
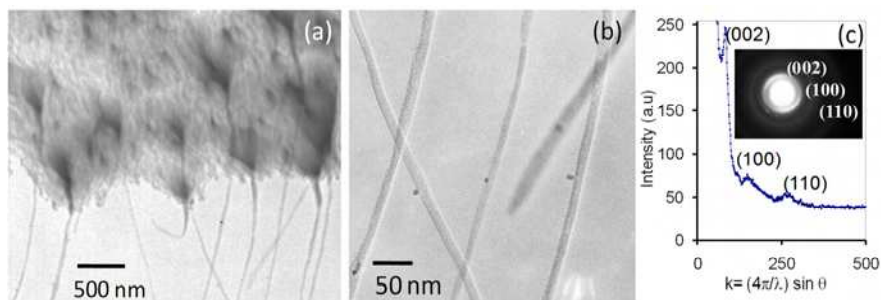

Fig. 4. HRTEM images of (a) transverse cross section of the C nanocluster-PI films (4.5 MeV Cu^{3+}, fluence 4 x 10^{14} ions cm^{-2}); (b) extended single ion-tracks with two tracks separated by a dielectric polymer barrier; and (c) SAED pattern obtained from the ion tracks.

Films irradiated at high fluence clearly provide multiple overlapping tracks that deviate from linear paths as seen in Fig. 4(a) of the HRTEM image of a microtomed cross-section which are consistent with SRIM track simulation (Ziegler et al., 2008). Fig. 4(a) illustrates the undulating pentration depth of the carbon nanocluster channels at the nanoscale due to the initial degree of planarity of the polymer film. Additionally, while the bulk of the ion tracks terminate at a depth between 4 and 4.5 μm, a small number of tracks extend well beyond this, penetrating deeper into the film due to subsequent irradiating ions following previously formed tracks, thereby loosing less energy during transmission. The widths of these single extended channels range between 15 and 25 nm (Fig. 4(b)) where one track can be seen passing in front of another separated by the dielectric polymer medium. Electron diffraction of the carbon clusters in the longitudinal cross-section of these channels (Fig. 4(c)) produces the (002), (100) and (110) rings indicating graphitic nanoclusters with basal spacings. The arc-shaped (002) diffraction ring is indicative of strong preferential orientation of these graphitic cluster layers parallel to the ion beam direction. This orientation could arise from relaxation processes to relieve the local surface stresses within the PI matrix during irradiation as well as forces exerted by the escaping volatile gases aligning the graphitic layers vertically to minimize flow resistance. Srivastava et al., determined the size of such carbon clusters by energy filtered TEM studies of ion irradiated polymer films supported on silicon to be ~5 nm in nanocolumns of ~10 nm diameter (Srivastava et al., 2006), although the planar carbon orientation was not identified.

Carbon bond hybridization is the other important aspect of electron transport by carbon nanocomposites as reflected in the ratio of sp^2 to sp^3 bonding. The low loss and carbon k-edge absorption in parallel electron energy loss spectra (PEELS) of these irradiated polyimide films (here fluence: 5×10^{14} ions cm^{-2}) reveals the presence of sp^2 π bonding in the ~6 eV absorption in the low loss region as well as sp^2 π* anti-bonding in the ~284 eV in the C-k edge region, as shown in Fig. 5(a) (i, ii) which arises from graphitic carbon clusters.

Notably Fig. 5(b) (i, ii) also shows the absence of π bonding in the un-irradiated polyimide films. However, a minor shoulder in the π* absorption region (~284 eV) is clear and arises from the aromatic rings of original PMDA-ODA polyimide molecules. These PEELS spectra of the irradiated films are similar to those obtained when graphitic nanoparticles are embedded in a similar polyimide film (Murugaraj et al., 2010) confirming the graphitic nature of the carbon clusters. Assuming these graphitic carbon nanoparticles possess total sp^2 bonding, the ratio of sp^2 to (sp^2+sp^3) carbon bonding in the un-irradiated and irradiated polyimide can be estimated as 0.074% and 94% respectively.
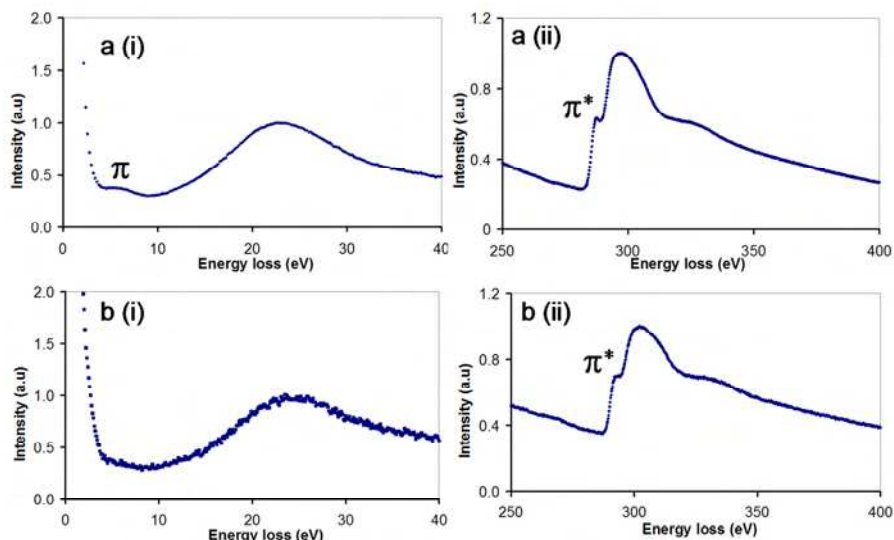
Fig. 5. Low loss (i) and carbon k-edge absorption (ii) spectra for: (a) irradiated polyimide film (fluence: 5.0×10^{14} ions cm^{-2}); and (b) pristine polyimide film.

In the single track regime, electron transport is predominantly along the tracks with negligible electronic conduction between the tracks due to the relatively large gaps between neighbouring tracks which would allow thermally activated electron tunneling at ambient temperatures. The electrical resistance of each track is independent of the fluence employed during formation. Along the tracks, the sole conduction mechanism is from electron hopping between carbon clusters within each track. Temperature dependent electron hopping is demonstrated in irradiated 5 μm thick polyimide films supported on gold coated substrates in the isolated ion track regime, where two slopes in the resistance plots during the heating cycle (Fig. 6) clearly indicate the influence of changing dielectric permittivity of the thermally altered polymer surrounding each track (Murugaraj et al., 2009a). The linear log resistance with T^{-1} indicates the dominant semiconducting behaviour of these conducting nanochannels. Hysteresis shown between the slopes of the heating and cooling cycles results from the thermal dissipation of the space charge in the region surrounding each track which accumulated at ambient conditions. Activation energies of these transport processes are provided by their respective slopes of Fig. 6(a-c). Here, the pronounced reduction in activation energies during heating results from dissipation of these space

charge effects. The influence of the increased dielectric permittivity seen on irradiation of these polymer films is analogous to bulk heterogeneous systems such as LiAlTi-phosphate with dispersed aluminum oxide (Kumar & Thokchom, 2007). The correlation of this dielectric permittivity enhancement with fluence of the irradiated films signifies a potential to control electron transport in these conducting nanowires by suitably tuning the space charge as well as the dielectric permittivity itself of the surrounding medium.
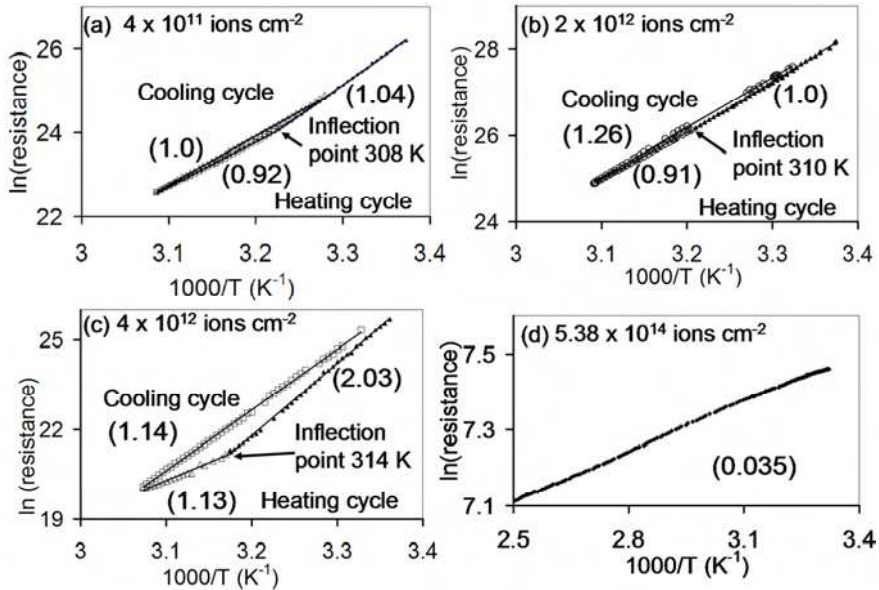
Fig. 6. Temperature dependent resistance of C nanocluster-PI films produced by irradiation: (a-c) irradiated with 55 MeV I^{+11} in the single track regime, and (d) PI film irradiated with 4.5 MeV Cu^{3+} ion in the track overlapping regime. Electron transport activation energies (eV) provided in brackets.

At still higher ion fluences, the multiple overlap regions produce bulk electron conductivity in PI films resulting from both hopping electron transport along the ion channels and electron tunning between neighbouring tracks due to their closer proximity. As irradiation is increased e.g from 9.00×10^{13} to 5.23×10^{14} ion cm^{-2}, the bulk electrical conductance increases from 3.33×10^{-9} to 1×10^{-4} siemens (Ω^{-1}) (Salvetat et al., 1997, Fink et al., 2008, Murugaraj et al., 2010). Their temperature dependence demonstrates Arrhenius thermal activation with conduction activation energy of ~35 meV, a value much smaller than that for the hopping conduction along such ion tracks (~1 eV) indicating the existence of an additional charge transport mechanism in these systems (Fig. 6(d)). That is, tunnelling of electrons in the multiple overlapping track regime provides an additional mode of the transport between neighbouring tracks when in close proximity. Fig. 7 shows schematically multiple overlapping ion tracks together with the conduction mechanisms. Interestingly, carbon nanotubes embedded in polymers provides a similar tunnelling process between neighbouring nanotubes for electron transport, although they are predominantly present as CNT bundles.
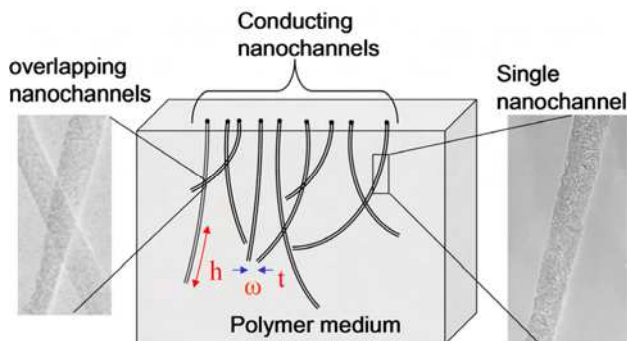
Fig. 7. Schematic of overlapping nanochannels in irradiated PI films showing hopping of electrons ('*h*') along the channels and tunnelling of electrons ('*t*') between neighbouring channels separated by a dielectric of thickness ('ω').

Here, Zhang et al. (2007) confirmed that a fluctuation induced tunneling (FIT) model fitted temperature dependent charge transport well in a functionalised multiwall CNT-polyurethan-urea composite examined. Subsequently, Hu et al. (2009) showed that the electrical resistance varied exponentially with variation of the tunnel gaps using an approach based on equivalent electrical circuits and classical modelling.
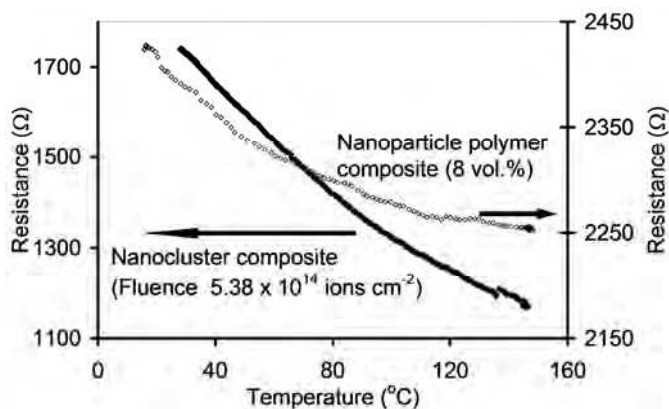
Fig. 8. Comparison of temperature dependent electrical transport of C nanoparticle-PI and C nanocluster-PI composite films.

When comparing the electrical resistance of polymer nanocomposite thin films formed by C nanoparticles and C nanocluster at volume fractions close to their respective percolation thresholds, both show an inverse temperature relationship characteristic of pronounced semiconducting behaviour. Fig. 8 demonstrates that the temperature dependence of the nanoparticle composite decreases with temperature and ultimately becoming independent typical of metallic-like scattering possibly from the nanoparticle aggregates. Whereas the nanocluster film has a significantly higher inverse temperature dependence confirming the absence of such charge scattering, indicating the ability of ion irradiation to produce more homogeneous nanocomposites with significantly lower degrees of aggregation.

3. Influence of imposed stresses

3.1 Thermal stresses

Three types of thermally induced stresses can be identified in carbon polymer nanocomposite thin films that influence the electron transport processes. Initial freestanding nanocomposite thin films prior to thermal annealing exhibit different temperature coefficients of resistance (TCR) which can be defined as the degree of the change of resistance for a given temperature change. The effect of annealing or thermal cycling is shown in Fig. 9 where it can be seen that initial heating to beyond ~90°C results in a coincident path with further heating and subsequent thermal cycling. That is, once annealed to this temperature, no hysteresis results in the electrical behaviour during thermal cycling. Annealing to ~90°C removes residual locked-in internal stresses in the film which results from molecular orientations created during the fabrication process, which in the case of these PI films involved thermal crosslinking at temperatures of 250°C.
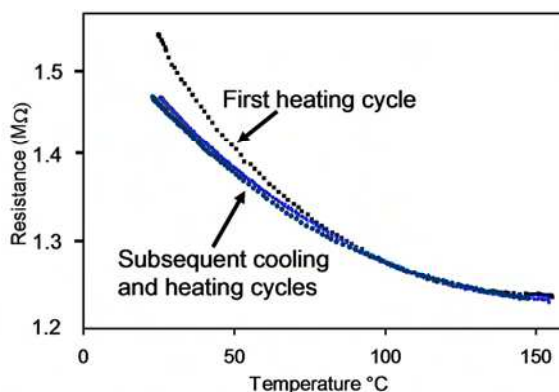

Fig. 9. Temperature dependent electrical resistance of freestanding nanoparticle-PI composite (5 vol% C) obtained during thermal annealing process.

Freestanding nanoparticulate composites also can potentially contain stresses arising from differences in the respective thermal expansion coefficient between the particle and the polymer components as discussed earlier. Thermal gradients can then induce considerable stresses within the interfacial region between particle and polymer medium which is highly dependent on the degree of molecular interaction or adhesion, and which can alter the electronic structure and the resulting electron transport. Murugaraj et al. (2008) examined impact of this effect in terms of the activation energies using Adkins model (1989).

Both nanoparticle and nanocluster composite films, when adhered to substrates, show an additional stress induced behaviour resulting from differential thermal expansion coefficients between the composite film and the substrate, which is reflected in the temperature dependent electrical behaviour of these systems. Fig. 10 shows the impact of nanoparticulate film adhesion to various substrates on the resistance ratios over a wide temperature range, where all these structures have semiconducting behaviour but with very differing negative temperature coefficient of resistance (NTCR) suggesting that the activation parameters for charge are influenced by this differential substrate adhesion. While the TCR for films adhered to rigid substrates (silicon and steel) were smaller than the freestanding film, the relative slopes clearly show that it is higher for the film fabricated on

the flexible polyimide substrates. Here, the lower NTCR of the rigidly supported films compared to the freestanding film arises from compressive stresses induced by the substrate on cooling during fabrication resulting in reduced tunnelling gaps through lower interparticle spacings. Nanocomposite films supported on flexible PI substrates experience an extensional deformation with temperature increasing the overall tunnelling gap distribution. Finite element analysis (ANSYS 9.0) of the impact of adhesion and changing temperature showed that stress peaks were very near the constrained (substrate) surface but importantly at a finite distance from it as shown in Fig. 11, which then gradually fall away towards the unconstrained surface (Murugaraj et al., 2008). The lower values of the stress just near the constrained surface suggest the presence of an interface that has material properties different to those of the film and substrate. Ding et al., using these techniques, modelled the micromechanical properties such as the shear and Young's modulus of this interfacial stress region and showed that they conformed to experimental data in terms of nanoparticle, polymer and volume fraction (Ding et al., 2008).
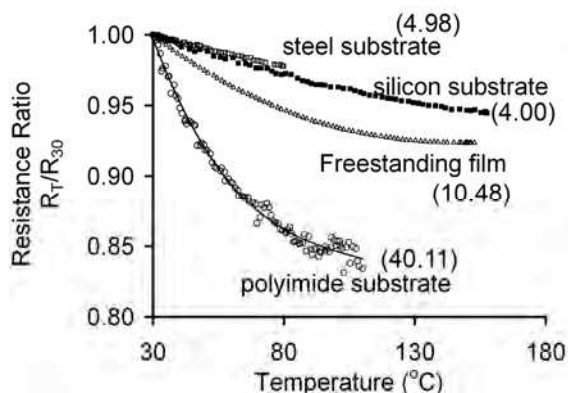

Fig. 10. Temperature dependent electrical resistance of 5 vol% C nanoparticle-PI film supported on various substrates and a freestanding film. Activation energies (meV) for electron transport provided in brackets.
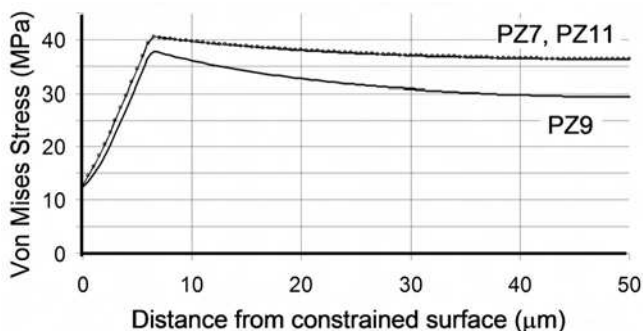

Fig. 11. Finite element analysis of the stress along the thickness of the C nanoparticle-PI film spin coated and cured on a rectangular silicon substrate (PZ9 along the corner, and PZ7 and PZ11 along the edges of the film).

3.2 Mechanical stresses

Conventional polymer composites above the percolation threshold respond non-linearly to the imposition of mechanical stresses due to the destruction and reformation of percolating conducting paths arising from physical contacts among the dispersed particle phase (Aneli et al., 1999b). As a result, their stress dependent resistance is largely confined to extensional deformations rather than compressional deformations. Here, large conducting paths exist where the electrons are delocalised over large atomic distances between, for example, carbon black aggregates, CNTs and dispersed metal islands, where the electron transport is highly dominated by large conducting segments (aggregates) rather than by hopping between well localised states (Sheng et al., 1978, Sheng, 1980). Below the percolation threshold, control of charge transport is critically dependent on electron hop distances or the tunnelling gaps and hence inter-particle spacings (Sheng et al., 1978, Sheng, 1980). When a particle polymer composite is subjected to compressive and extensional stresses, spatial rearrangement of the particles dispersed in the polymer matrix occurs which impacts on the electron transport and the measured electrical conductivity.
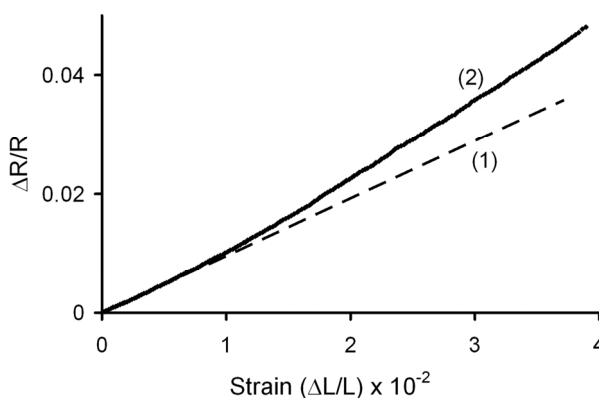

Fig. 12. Electromechanical response of nanoparticle-polyimide composite thin films: (1) and (2) with C vol% 3.0 and 8.0, respectively.

Nanoparticle – polymer composite films demonstrate similar percolation behaviour in their electrical conductivity although the transition occurs at considerably lower particle volume fractions due to the increased number of potential particle contacts. The prevalent charge transport mechanisms operating are also similar to conventional polymer composites both above and below the nanoparticle percolation threshold (Shekhar et al., 2006a). The electrical response to deformation or electromechanical behaviour of freestanding nanocomposite films show a linear response across a wide range of strains when operating well below the percolation threshold as seen in Fig. 12. Approaching the threshold, the response tends to become non-linear (Murugaraj et al., 2009b), while above it, considerable non-linearity is consistently seen. The relative dimensions of these nanoparticle films themselves influence the strain response significantly due to the effect of differential changes in interparticle spacings laterally along the strain axis and transversely across it, as a result of the Poisson's ratio during deformation. Under such an imposed process, lateral extension increases the resistance ratio while transverse contraction tends to reduce it. Fig. 13 shows that as the

transverse width of the film decreases, the electromechanical response increases significantly due to these competing effects (Murugaraj et al., 2009b). Fig. 13 also indicates that when the film is adhered to a rigid substrate, the lateral contraction is significantly reduced, which yields an overall increase in electromechanical response. Nanoparticle – polymer films below the percolation threshold clearly demonstrate that the electromechanical response to both extensional and compressive deformation are equivalent, as shown in Fig. 14 since relative particle distances is the primary determinant of electrical response.
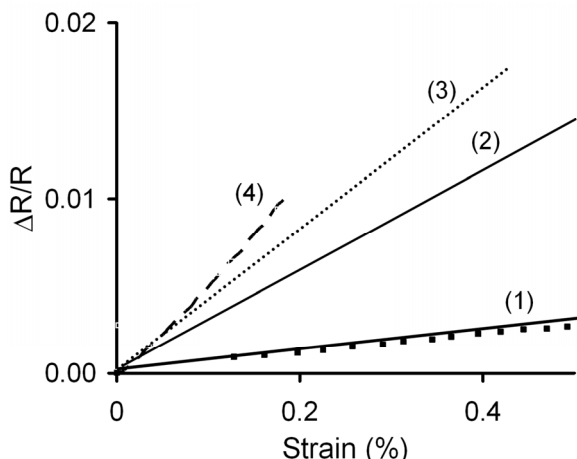

Fig. 13. Electromechanical responses of 8 vol% C nanoparticle-PI freestanding film strips of length 2.2 mm thickness 90 μm: (1), (2) and (3) widths 2.0, 1.0 and 0.7 mm, respectively; (4) Electromechanical response obtained on a similar steel supported film of width 1.5 mm.
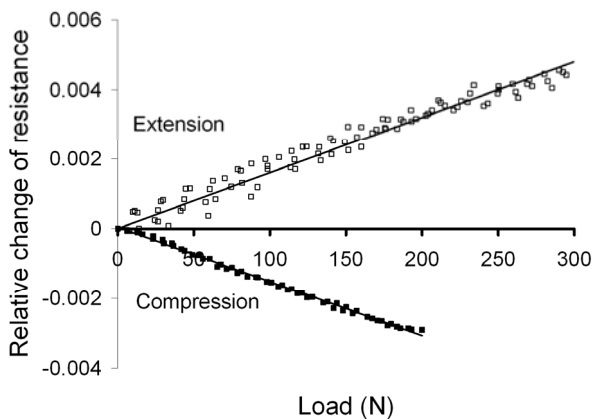

Fig. 14. Electromechanical response of a 5 vol% C nanoparticle-PI film adhered to a carbon fibre composite substrate under extensional and compressive strains.
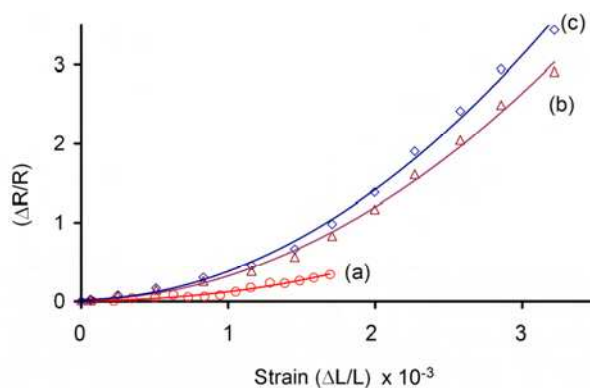
Fig. 15. Electromechanical response of C nanocluster-PI composites fabricated with fluences: (a) 3.28×10^{14}, (b) 5.00×10^{14}, and (c) 5.23×10^{14} ions cm^{-2}.

Irradiation of polymer films inherently produce anisotropic composites with orientated channels consisting of carbon nanoclusters in the ion beam direction. Unlike the dispersed nanoparticle composites, electron transport in these anisotropic nanocluster polymer films occurs through electron hopping across the carbon clusters within the nanochannels together with lateral inter-channel tunnelling as illustrated in Fig. 7. The electrical response to mechanical stress of these films exceeds nanoparticulate films by two orders of magnitude due to the exponential relationship of conductivity to electron tunnelling gap distances shown in Fig. 15. This also indicates that increasing the ion irradiation (fluence) increases the volume fraction of these orientated channels and greatly enhanced electromechanical responses (Murugaraj et al., 2010b). Carbon nanotube – polymer systems, although a similar high aspect ratio nanocomposite, show much reduced electromechanical sensitivities due their inherent random orientations within the three dimensional polymer matrix which results in a wider size dispersion of conducting regions as well as wider variations in the tunnelling gaps between adjacent nanotubes (Zhang et al., 2007, Hu et al., 2009). Whereas, the narrow distribution of tunnelling gaps in the ordered nanocluster composites provides their unique electromechanical enhancement.

3.3 Interfacial adhesion

The interfacial adhesion of polymers is essential for all polymeric devices in electronic applications, particularly those involved in structural sensing devices where the transmission of stress over a wide temperature range is fundamental. The use of conventional polymers such as the polyimides in electronic devices often results in poor adhesion as well as thermal and stiffness mismatches which generate high interfacial stresses resulting in displacements, cracks and delamination (Ho et al., 1989, Ree et al., 1992). Crosslinked polyimides are known to posses weak adhesion characteristics due to stiff molecular chains, closed imide rings and a lack of hydrogen bonding functionality shown by such adhesives as the cyanoacrylates (Ree et al. 1992). In polyimides generally and polyimide based composite films residual stresses due to imperfect adhesion can vary their functional properties such as dielectric constant and electron transport when used as both active and passive device components.

The modification of the polymer surfaces to promote adhesion uses either physical processes including ion beam, photografting, plasma etching, corona discharge and sputtering or chemical treatments such as etching with potassium or ammonium hydroxides and ethylene diamine (Ranucci et al., 2001, Park et al., 2007, Kim et al., 2005, Butoi et al., 2001, Lin et al., 2005). Physical treatments often introduce foreign materials into interfaces which may result in reliability failures whereas chemical based processes, if well controlled, confine reactions to the surface resulting in a more homogenous modification (Lin et al., 2005). Polymer composites, being a biphasic system, add additional complexity to surface treatments needed to enhance interfacial adhesion. Surface treatment, such as etching not only modifies the microstructure but alters the chemical functionality within the interfacial region which may be either the continuous polymer medium or the exposed nanoparticle component. Fig. 16 illustrates the effect of KOH etching on surface microstructure of a carbon nanoparticle – polyimide composite film. Here, the development of surface trenches within the polymer is apparent as etching proceeds, which is followed by increased exposure of the carbon nanoparticles in the final surface (Murugaraj et al., 2010a). The resulting topological structure as well as the chemical modification can be determined by friction force AFM microscopy using a hydrophilic probe in the contact mode to provide imaging and chemical adhesion characteristics simultaneously. Fig. 17(a) shows the topographic image of an etched composite surface where the exposed carbon nanoparticles are visualised together with their heights of about 10-20 nm by line analysis (Murugaraj et al., 2010a). Friction force images of the same area provide information that can be correlated with the wetting and adhesion characteristics of the surface. Fig. 17(b) shows the 3-D image of the lateral force scan, where frictional forces appear to be less over the exposed carbon nanoparticles compared to the surrounding polyimide surface. Since the contact mode AFM tip generates a stronger friction force on more hydrophilic areas, it indicates that the PI polymer surface undergoes significantly greater chemical modification to include polar groups than the exposed carbon nanoparticle areas. Since friction force microscopy provides both microstructural and functional information at the nanoscale, it complements bulk techniques such as FTIR and contact angle measurements particularly when biphasic nanocomposite surfaces are encountered.
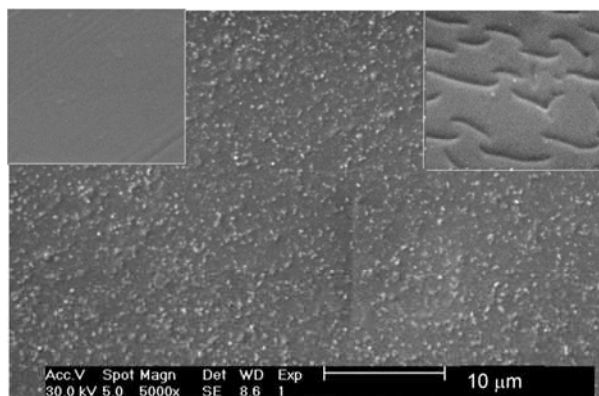

Fig. 16. SEM image of C nanoparticle-PI composite surface treated with 3.0 M KOH at 25 °C for 9 min. Inset on left is untreated composite film surface and on right is composite film treated with 0.1 M KOH at 80 °C for 30 min.
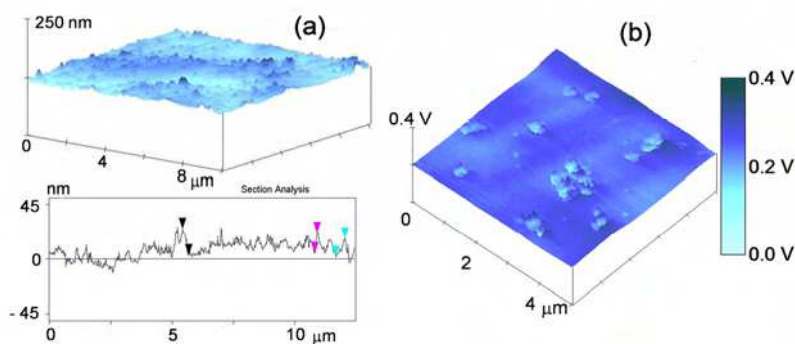
Fig. 17. AFM images of the C nanoparticle-PI composite surface after 3.0 M KOH at 25 °C for 9 min: (a) height scan and (b) friction force.

4. Dielectric behaviour of nanocomposites

Conventional polymer composites employing conductive particles have been shown by Rao & Wong (2002) to behave as a cascade of capacitors connected in series and parallel operating through space charge polarization to achieve increased effective dielectric constants at conductive particle volume fractions close to but not exceeding the percolation threshold. Additionally the dielectric constant of polymer composites has been increased by the incorporation of high dielectric particles such as barium titanate, lead magnesium niobate-lead titanate and titanium dioxide (Rao et al., 2002, Rao & Wong, 2004, Ulrich, 2004, Bai et al., 2000, Liou & Chiou, 1998). Such polymer composites obey Maxwells's mixing rule (Garnett, 1904), where the composite dielectric constant is a linear function of the volume fraction of the two components. Lewis (2005) has recently reviewed the role of nanoparticle interfaces in the dielectric behaviour of nanocomposites in both passive interface systems where the response to the applied electrical field is within the electrical double layer (EDL) and active interface systems where the response is piezomechanical.

Particulate nanocomposites, on the other hand, can exhibit considerably different behaviour in their dielectric permittivities ($\varepsilon_{composite}$) to that predicted by Maxwell's mixing rule for dielectric composites when below their percolation thresholds. Whereas reductions in $\varepsilon_{composite}$ occur when the surface functionality of the nanoparticles such as hydroxyl groups reduce the polymer density and thereby decrease the real part of the dielectric permittivity (Nelson & Fothergill, 2004). Significant enhancement, beyond that predicted by Maxwell's rule, can originate from specific physicochemical interactions between the nanoparticle and the polymer within the interfacial region which provide additional contributions to the overall polarizability (Murugaraj et al., 2005). Such nanocomposites have $\varepsilon_{polymer} < \varepsilon_{particle} < \varepsilon_{composite}$ in contrast to the conventional composites above where $\varepsilon_{polymer} < \varepsilon_{composite} < \varepsilon_{particle}$ which in nanosystems becomes a dominant effect due to greatly increased interfacial surface area above certain volume fractions.

Dielectric nanocomposite thin films consisting of alumina ($\varepsilon = 9.8$) or silica ($\varepsilon = 3.6$) nanoparticles dispersed in polyimide ($\varepsilon = 3.5$) show this monotonically increasing enhancement with increasing nanoparticle content as indicated in Fig. 18. The resultant $\varepsilon_{composite}$ of these systems is independent of frequency up to 10 MHz indicative of its origin as

dipolar contributions rather than space charge polarization commonly observed in metal particle composites (Rao et al 2002). Vo and Shi (Vo & Shi, 2002, Todd & Shi, 2003) showed in physical modeling that enhanced dielectric permittivity arise from the interphase region considered as a unique phase with a different dielectric constant depending on particle concentration and size as well as the interaction with the polymer. Fitting the data from the nanoparticle – PI systems to these physical models yields a dielectric permittivity of the interface $\varepsilon_{interface}$ of 280 for the alumina nanocomposites and 19 for their silica counterparts (Murugaraj et al., 2005).
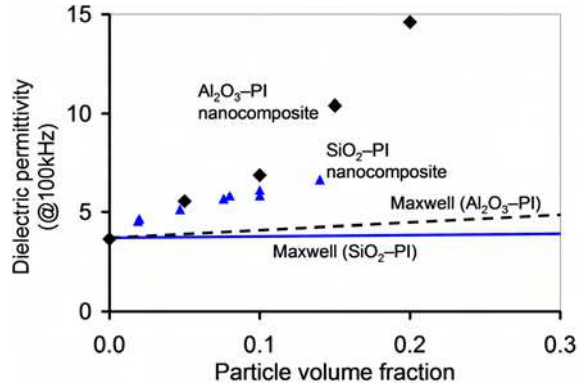

Fig. 18. Composite dielectric permittivity with alumina and silica nanoparticle contents measured at 100 kHz and 25 °C.
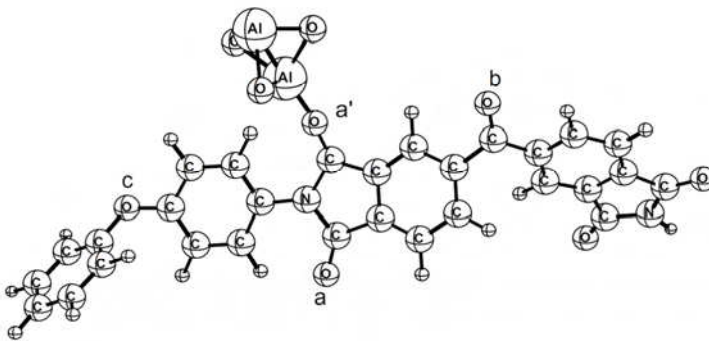

Fig. 19. Optimized molecular structure of the PI unit and interaction with the aluminium: (i) on the carbonyl group of the five membered ring (a and a'), (ii) on the carbonyl group in the chain (*b*) and (iii) the ether oxygen (*c*).

The mechanisms that lead to this enhancement of $\varepsilon_{interface}$ have been examined with *ab initio* molecular orbital calculations of the molecular interactions in the interfacial region. For the alumina – PI system these calculations predict the existence of a strong electrostatic attraction between the positively charged aluminium and the negative oxygens of the polymer functionality leading to polarization of the system and an enhanced dielectric response as illustrated in Fig. 19 (Jacob et al., 2009). The oxygen atoms therefore play a dual

role involving covalent bonding with the polymer chain functionality as well as electrostatic interactions with the alumina nanoparticles (Jacob et al. 2009). Shi and Ramprasad (2007, 2008) examined the silica – polymer system using density functional theory (DFT) and provided a spatial profile of the dielectric constant within the interfacial regions, such that calculated optical and static dielectric constants were in close agreement with those determined experimentally.

5. Applications of electron conduction

5.1 Structural health monitoring

Monitoring and thus control of the structural health of critical infrastructure for safety and security as well as economic efficiency is increasingly becoming an important aspect of industrial, defence and national infrastructure. This structural monitoring requires the identification of detrimental changes to the material performance of infrastructure in its current state (diagnostic analysis) or its future condition (prognostic analysis). As such, the current time-based mode of structural and mechanical maintenance is slowly giving way to more cost effective condition based maintenance (Farrar & Worden, 2007). Material changes occur at the local scale within the microstructure which may not be adequately monitored by conventional strain sensors that essentially respond to the overall system. Sensing localised 2-D stress fields requires a high density of direct strain measurements (Loh et al., 2008), which for conventional strain gauges makes the overall systems operationally obtrusive. Increased emphasis is also being given to densely embedded monitoring systems potentially able to utilize wireless interrogation for data transfer (Lynch et al., 2007, Jia & Sun, 2006).
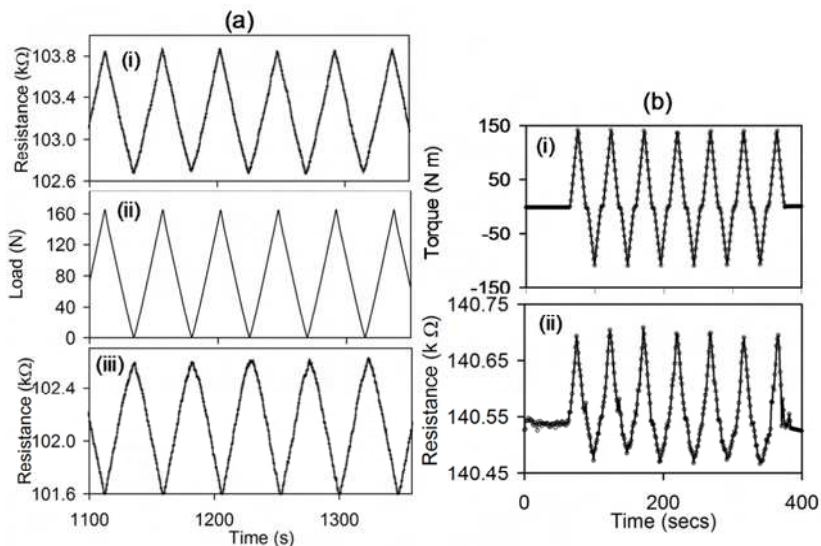

Fig. 20. Electrical resistance of 5 vol% C nanoparticle-PI strain sensing element, (a) cyclic loading: (i) extensional, (iii) compressional deformation, and (ii) is applied cyclic load; (b) cyclic torsional deformation: (i) applied torque and (ii) corresponding resistance.

Polymer based embedded strain monitoring devices such as carbon nanoparticle and CNT nanocomposites are a growing area to meet these demands (Kang et al., 2009, Loh et al., 2007) since they can be fabricated into a variety of structures including 2-D arrays. Carbon nanoparticle films acting as strain sensors can tolerate applied deformations of ±40,000 μstrains (Murugaraj et al., 2009b) where they show a proportional linear response to deformation, in comparison to conventional metal foil and semiconductor based strain sensing elements which are limited to ~10,000 μstrains. Such polymer based sensing films when subjected to cyclic aging exceeding 500 cycles show electromechanical responses that remain in phase with the imposed deformation indicating the absence of material degradation as shown in Fig. 20(a). Also, the electromechanical sensitivity in both extension and compression is equivalent as shown this in Figure, which allows these films to also act as a single element for direct torque measurements (Mainwaring et al., 2008). Fig. 20(b) demonstrates the quantitative relationship between an applied cyclic torque and the measured electrical response. Here it can be seen that this type of nanocomposite is able to electrically track the angular deformation through the whole cycle directly, again without hysteresis, for prolonged periods. Nanoparticle – polymer films having electrical resistances of the order kOhms reduce the power requirements for interrogation by more than two orders of magnitude permitting multiple strain sensors to be used in 2-D strain mapping with minimal electrical interference and joule heating (Mainwaring et al., 2008).

In comparison to nanoparticle composite films, nanocluster films demonstrate electromechanical sensitivities that are two orders of magnitude greater as noted previously, and hence provide proportional increases in strain sensitivities when used in sensing devices. The relative strain sensing response of conventional metal foil gauges, carbon nanoparticle and nanocluster composite films are shown in Fig. 21.
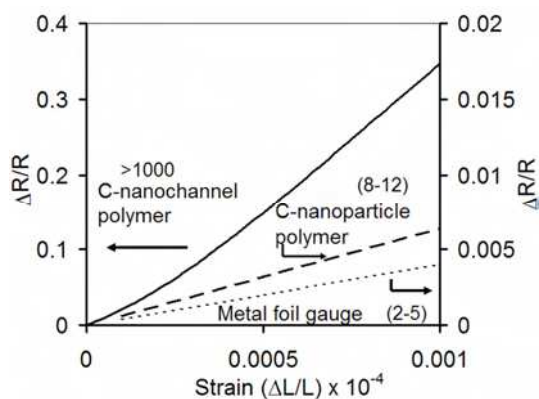

Fig. 21. Electromechanical sensitivities of 3 strain gauge materials, with relative sensing gauge factors in brackets.

5.2 Thermal sensing

Conductive polymer nanocomposite films, whether containing carbon or metal particles exhibit either a positive temperature coefficient of resistance (PTCR) or a negative coefficient (NTCR) depending on the nanoparticle volume fraction. Above the percolation threshold PTCR behaviour has been exploited in such applications as switching and current protection

devices and as well as self regulating heater elements (Boiteux et al., 1999). This positive behaviour is also employed in electromagnetic shielding applications (Bigg, 1984) due its metal-like conduction behaviour. In the non-percolating regime nanocomposites have a NTCR due to their semiconducting nature and therefore show good potential for flexible environmentally robust thermal sensing applications (Murugaraj et al., 2006a, 2006b), rather than ceramic based sensors.

Fig. 22(a) shows the behaviour of the C-nanoparticle polyimide films below the percolation threshold (≤ 8 vol %). Here, the two common parameters characteristic of thermistor performance are the thermal sensitivity 'α' and sensitivity index 'β' as given by:

$$\alpha = \frac{1}{R_T}\frac{dR}{dT}\times 100 \qquad (9)$$

$$\beta = \frac{\ln\left(\dfrac{R_1}{R_2}\right)}{\dfrac{1}{T_1}-\dfrac{1}{T_2}} \qquad (10)$$

where R_T is the resistance at temperature T, and R_1 and R_2 are the resistances at temperature T_1 and T_2 respectively. The thermal sensitivity 'α' decreases with increasing carbon content due to decreased activation energies at higher volume fractions. Charge carrier or metallic scattering also influences the thermal sensitivity due to increased aggregation at higher carbon fractions while still below the percolation threshold and increased temperatures (<100°C). In contrast, the thermal sensitivity of carbon nanocluster composite films remains constant over a wide temperature range due to the minimum aggregation of such clusters thereby reducing the intraparticle scattering (Murugaraj et al., 2006a and 2006b).
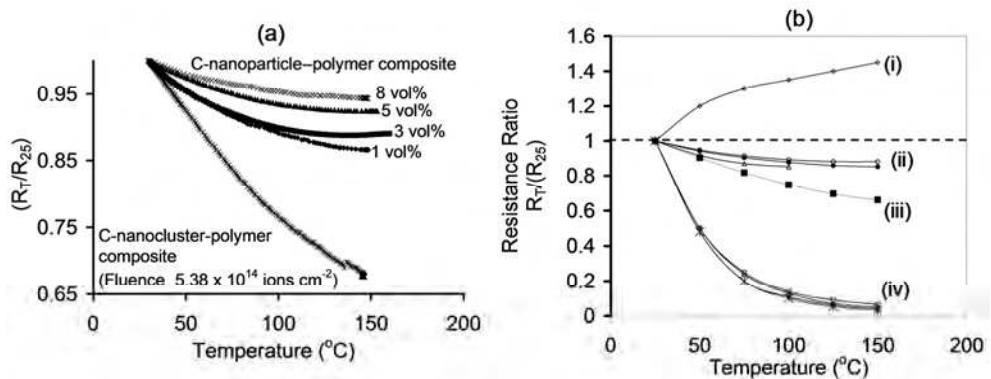

Fig. 22. (a) Resistance ratio of C nanoparticle-PI films and a C nanocluster composite film; and (b) Resistance ratio for different thermistor elements: (i) platinum resistor thermometer (Thermometrics), (ii) C nanoparticle-PI NTC thermistors, (iii) C nanocluster-PI thermistor, and (iv) commercial oxide NTC thermistors (Betatherm).

Fig. 22(b) compares the resistance ratio of polymer nanocomposite thermistor films to conventional thermistor devices. Thermal sensitivities of polymer nanocomposite films fall in the range -0.09 to -0.40 %K^{-1} with the respective sensitivity indices in the range 95 to 390 K. Whereas ceramic NTC thermistors have α and β values in the range –3 %K^{-1} to –6 %K^{-1} and 3000 K to 4000 K respectively (Rousset et al., 1994). Such differences in performance arise from the lower activation energies for electron transport associated with carbon nanocomposite films.

6. Conclusions and future perspectives

Carbon polymer nanocomposites can be produced using ex-situ nanoparticle dispersion within polymer monomers followed by crosslinking to yield highly distributed systems. Alternatively, carbon nanocluster films can be produced in-situ by ion beam irradiation which yields high aspect ratio nanostructures separated by a unaltered dielectric polymer medium. Both systems obey Mott's variable range electron hopping mechanism, but the irradiated nanocluster composites provide an addition mode of charge transfer due to electron tunnelling between isolated nanocluster channels within close proximity. Hence their sensitivity to mechanical deformation is two orders of magnitude higher than the equivalent nanoparticle composites. Electron transport along these nanochannels is modulated by changes in the dielectric behaviour of the immediately surrounding polymer. The dielectric permittivity of nanocomposites can also be locally altered through molecular scale physiochemical interactions between polymer chains and the high surface area of nanoparticles forming the interfacial region. Such carbon nanocomposite films respond to imposed stimuli such as mechanical and thermal stresses allowing their use in various sensing devices. The ability to tune the dielectric characteristics at the nanoscale allows control of electron flow opening new possibilities and novel electronic functionalities not achievable in conventional bulk materials.

7. Acknowledgements

8. References

Adkins, C.J. (1987). Conduction in granular metals with potential disorder. *J. Phys. C: Solid State Physics*, 20, 235-244, ISSN 0022-3719

Adkins, C.J. (1989). Conduction in granular metals-variable range hopping in a coulomb gap? *J. Phys. Conden. Mater.* 29, 1253-1259, ISSN 0953-8984

Adla, A.; Fuess, H. & Trautmann, C. (2003). Characterisation of heavy ion tracks in polymers by transmission electron microscopy. *J. Polym. Sci. Part B: Polym. Phys.* 41, 2892-2901, ISSN 0887-6266

Aneli, J. N.; Zaikov, G. E. & Khananashvili, L. M. (1999a). Effects of mechanical deformations on the structurization and electric conductivity of electric conducting polymer composites. *J. Appl. Polym. Sci.,* 74, 601-621, ISSN 0021-8995

Aneli, J. N.; Zaikov, G. E. & Khananashvili, L. M. (1999b). Effects of mechanical deformations on the structurization and electrical conductivity of polymer composites. *Int. J. Polym. Mater.,* 43, 19-61, ISSN 0091-4037

Bai, Y.; Cheng, Z-Y.; Bharti, V.; Xu, H. & Zhang, Q. M. (2000). High-dielectric-constant ceramic-powder polymer composites. *Appl. Phys. Lett.,* 76, 3804-3807, ISSN 0003-6951

Betatherm, www.betatherm.com/news/db/pdf/1102338840.pdf

Bigg, D. M. (1984). An investigation of the effect of carbon black structure, polymer morphology, and processing history on the electrical conductivity of carbon-black-filled thermoplastics. *J. Rheology*, 28, 501-516 ISSN 0148-6055

Boiteux, G.; Fournier, J.; Issotier, D.; Seytre, G.; Marichy, G. (1999). Conductive thermoset composites: PTC effect. *Synthetic Metals*, 102, 1234-1235, ISSN 0379-6779

Butoi, C. I.; Steen, M. L.; Peers, J. R. D. & Fisher, E. R. (2001). Mechanisms and energy transfer for surface generation of NH_2 during NH_3 plasma processing of metal and polymer substrates. *J. Phys. Chem.B,* 105, 5957-5967, ISSN 1089-5647

Chui, T.; Deutscher, G.; Lindenfeld, P. & McLean, W.L. (1981). Conduction in Granular aluminium near metal-insulator transition. *Phy. Rev. B : Condens. Mater.,* 23, 6172-6175, ISSN 0163-1829

Costantini, J.-M.; Couvreur, F.; Salvetat, J.-P. & Bouffard, S. (2002). Micro-Raman study of the carbonization of polyimide induced by swift heavy ion irradiations. *Nucl. Instrum. Methods Phys. Res. Sect. B*, 194, 132-140, ISSN 0168-583x

Davenas, J. Boiteux G.; Xu, X. L. & Adem, E. (1988). Role of the modifications induced by ion beam irradiation in the optical and conducting properties of polyimide. *Nucl. Instrum. Methods Phys. Res. Sect. B,* 32, 136-141 ISSN 0168-583x

De Bonis, A.; Bearzotti A. & Marletta, G. (1999). Structural modifications and electrical properties in ion-irradiated polyimide. *Nucl. Instrum. Methods Phys. Res. Sect. B*, 151, 101-108, ISSN 0168-583x

Devenyi, A.; Manaila-Devenyi, R. & Hill, R.M. (1972). Hopping conduction through localised states in Nb/Al_2O_3 films. *Phy. Rev. Letts.,* 29, 1738-1741, ISSN 0031-9007

Ding, Y.; Tran, K.N.; Gear, J.A.; Mainwaring, D. & Murugaraj, P. (2008). The influence of interphase between nanoparticles and matrix on Young's Modulus of nanocomposites. *Proceedings of the International Conference on Nanoscience and Nanotechnology (ICONN2008)*, pp. 28-31, ISBN 1424415047, Melbourne, Australia, 25-29 February 2008, IEEE Publishing Co., Piscataway, NJ (USA)

Di Gianni, A.; Trabelsi, S.; Rizza, G.; Sangermano, M.; Althues, H.; Kaskel, S.& Voit, B. (2007). Hyperbranched polymer/T_iO_2 hybrid nanoparticles synthesized via an in situ sol-gel process. *Macromol. Chem. Phys.,* 208, 76–86, ISSN 1022-1352

Di Girolamo, G.; Massaro, N.; Piscopiello, M. & Tapfer, L. (2010). Metal ion implantation in inert polymers for strain gauge applications. *Nucl. Instrum. Methods Phys. Res. Sect. B*, 268, 2878–2882, ISSN 0168-583X

Efros, A.L. & Shklovskii, B.I. (1975). Coulomb gap and low temperature conductivity of disordered systems. *J. Phys. C,* 8, L49-L51, ISSN 0022-3719

Efros, A.L. (1976). Coulomb gap in disordered systems. *J. Phys. C,* 9, 2021-2030, ISSN 0022-3179

Entin-Wohlman, O.; Gefen Y. & Shapira, Y. (1983). Variable-range hopping conductivity in granular materials. *J Phys. C,* 16, 1161-1167, ISSN 0022-3719

Farrar, C. R. & Worden, K. (2007). An introduction to structural health monitoring. *Philos. Transact. A: Math. Phys. Eng. Sci.*, 365, 303-315, ISSN 1471-2962

Feurer, T.; Sauerbrey, R.; Smayling M.C. & Story, B.J. (1993). Ultraviolet-laser-induced permanent electrical conductivity in polyimide. *Appl. Phys. A,* 56, 275-278, ISSN 721-7250

Fink, D.; Hu, H.; Klett, R.; Mueller, M.; Zhu, J.; Li, C.; Sun, Y.; Ma, F. & Wang, L. (1995). Conductivity of aged non-overlapping and overlapping tracks in ion irradiated polyimide. *Radiat. Meas.,* 25, 51-54, ISSN 1350-4487

Fink, D.; Klett, R.; Chadderton, L.T.; Cardoso, J.; Montiel, R.; Vazquez, H. & Karanovich, A. A. (1996). Carbonaceous clusters in irradiated polymers as revealed by small angle X-ray scattering and ESR. *Nucl. Instrum. Methods Phys. Res. Sect. B*, 111, 303-314, ISSN 0168-583x

Fink, D.; Chandra, A.; Fahrner, W.R.; Hoppe, K.; Winkelmann, H. Saad, A.; Alegaonkar, P.; Berdinsky, A.; Grasser, D. & Lorenz, R. (2008). Ion track -based electronic elements. *Vacuum*, 82, 900-905, ISSN 0042-207x

Fragala, M. E.; Compagnini, G.; Licciardello, A. & Puglisi, O. (1998). Track overlap regime in ion-irradiated PMMA. *J. Polym. Sci. Part B: Polym. Phys.,* 36, 655-644, ISSN 0887-6266

Fournier, J.; Boiteix, B., Seytre, G. & Marichy, G. (1997). Positive temperature coeffficient in carbon black/epoxy polymer composites. *J. Mater. Sci. Lett.,* 16, 1677-1679, ISSN 0261-8028

Garnett, J. C. M. (1904). Colours in metal glasses and in metallic films. *Phil. Trans. Royal Soc. A*:, 203, 385-420, ISSN 1364-503X

Garnier, F. (1998). Thin film transistors based on organic conjugated semiconductors. *Chem. Phys.* 227, 253-262, ISSN 0301-0104

Groehn, F.; Kim, G.; Bauer, B.J. & Amis, E.J. (2001). Nanoparticle formation within dendrimer-containing polymer networks: Route to new organic-inorganic hybrid materials. *Macromolecules, 34,* 2179-2185, ISSN 0024-9297

Grytsenko, K.P. & Schrader, S. (2005) Nanoclusters in polymer matrices prepared by co-deposition from a gas phase. *Adv. Colloid Interface Sci.,* 116, 263–276, ISSN 0001-8686

Hanemann, T. & Szabó, D.V. (2010). Polymer-nanoparticle composites: From synthesis to modern applications. *Materials, 3,* 3468-3517, ISSN 1996-1944

Hatchett, D. W. & Josowicz, M. (2008). Composites of intrinsically conducting polymers as sensing nanomaterials. *Chem. Rev.,* 108, 746-769, ISSN 0009-2665

Hioki, T.; Noda, S.; Kakeno, M.; Yamada, K. & Kawamoto, J. (1983). Electrical and optical properties of ion - irradiated organic polymer Kapton H. *Appl. Phys. Lett.,* 43, 30-32, ISSN 0003-6951

Ho, P. S. (1989). Chemistry and adhesion of metal-polymer interfaces. *Appl. Surf. Sci.* 41/42, 559-566, ISSN 0169-4332

Hu, N.; Karube, Y.; Yan, C.; Masuda, Z. & Fukunaga, H. (2009). Tunneling effect in a polymer/carbon nanotube nanocomposite strain sensor. *Acta Mater.* 56, 2929-2936, ISSN 1359-6454

Jacob, R.; Jacob, A.P. & Mainwaring, D.E. (2009). Mechanism of the dielectric enhancement in polymer–alumina nano-particle composites. *J. Mol. Struct.,* 933, 77–85, ISSN 0022-2860

Jena, P.; Khanna, S. N. & Rao, B. K. (2001). The role of interface on the properties of cluster assemblies. *J. Cluster Sci.,* 12(3), 443-456, ISSN 1040-7278

Jia, Y. & Sun, K. (2006). Thick film wireless and powerless strain sensor. *Proc. SPIE-Int. Soc. Opt. Eng.,* 6174, 61740Z/1-61740Z/11, ISSN 0277-2668

Kafafi, S.A.; LaFemina, J.P. & Nauss, J.L. (1990). Electronic structure and conformation of polymers from cluster molecular orbital and molecular mechanics calculations: Polyimide. *J. Am. Chem. Soc.,* 112, 8742–8746, ISSN 0002-7863

Kaiser, A.B. (2001). Systematic conductivity behaviour in conducting polymers: Effects of heterogeneous disorder. *Adv. Mater.,* 13, 927-941, ISSN 0935-9648

Kang, J.H.; Park, C.I.; Scholl, J.A.; Brazin, A.H.; Holloway, N.M.; High, J.W.; Lowther, S. E. & Harrison, J. S. (2009). Piezoelectric characteristics of single wall carbon nanotube/polyimide nanocomposites. *J. Polym. Sci. Part B: Polym. Phys.,* 47, 994-1003, ISSN 0887-6266

Kim, S-H.; Cho, S.H.; Lee, N-E.; Kim, H.M.; Nam, Y. W. & Kim, Y-H. (2005). Adhesion properties of Cu/Cr films on polyimide substrate treated by dielectric barrier discharge plasma *Surf. Coat. Technol.,* 193, 101-106, ISSN 0257-8972

Klafter, J. & Sheng, P. (1984). The coulomb gap and the metal-insulator transition in granular films. *J Phys. C,* 17, L93-L96, ISSN 0022-3719

Klemens, P.G. (1986). Thermal expansion of composites. *Int. J. Thermophy.,* 7, 197-206, ISSN 0195-928X

Kryszewski, M. & Jeszka, J. (2003). Charge carrier transport in heterogeneous conducting polymer materials. *Macromol Symp.* 194, 75-86, ISSN 1022-1360

Kumar, B. & Thokchom, J. S. (2007). Space charge signature and its effects on ionic transport in heterogeneous solids. *J. Am. Ceram. Soc.,* 90, 3323-3325, ISSN 0002-7820

Lewis, T. J. (2005). Interfaces: nanometric dielectrics. *J. Phys.D: Appl. Phys.,* 38, 202-212, ISSN 0022-3727 and references therein

Lin, Y-S.; Liu, H-M.& Tsai, C-W. (2005). Nitrogen plasma modification on polyimide films for copper metallization on microelectronic flex substrates *J. Polym Sci. Pt. B: Polym. Phys.,* 43, 2023-2038, ISSN 0887-6266

Liou, J. W. & Chiou, B. S. (1998). Dielectric tunability of barium strontium titanate/silicone-rubber composite. *J. Phys. Condensed Matter.,* 10, 2773-2786, ISSN 0953-8984

Loh, K.J.; Kim, J.; Lynch, J.P.; Kam, N.W.S. & Kotov, N.A. (2007). Multifunctional layer by layer carbon nanotube-polyelectrolyte thin films for strain and corrosion sensing. *Smart Mater. Struct.,* 16, 429-438, ISSN 0964-1726

Loh, K. J.; Lynch, J. P.; Shim, B. S. & Kotov, N. A. (2008). Tailoring piezoresistive sensitivity of multilayer carbon nanotube composite strain sensors. *J. Intell. Mater. Struct.,* 19, 747-764, ISSN 1045-389X

Lynch, J. P. (2007). An overview of wireless structural health monitoring for civil structures. *Philos. Transact. A: Math. Phys Eng. Sci.,* 365, 345-372, ISSN 1364-503X

Mainwaring, D.; Murugaraj, P.; Mora-Huertas, N. & Sethupathi, K. (2008). Enhanced electromechanical response of nonpercolating polymer-nanoparticle composite films. *Appl. Phys. Lett.* 92 (25), 253303/1-253303/3, ISSN 0003-6951

McAlister, S.P.; Inglis, A.D. & Kroeker, D.R. (1984). Crossover between hopping and tunnelling conduction in Au-SiO$_2$ films. *J. Phys C* 17 (1984). L751-L755, ISSN 0022-3719

Mora-Huertas, N.E.; Murugaraj, P. & Mainwaring, D.E. (2004). Temperature-dependent transport properties in the semiconducting regime of nanoparticle carbon-

polyimide composite films. *Physica E (Amsterdam, Neth.),* 24, 119-123, ISSN 1386-9477

Mott, N.F. (1969). Conduction in noncrystalline materials. *Phi. Mag.*, 19, 160, 835-852, ISSN 0031-8086

Mott, N.F. & Davis, E.A. (1978). *International Series of Monographs on Physics. Electronic Processes in Non-Crystalline Materials.* Oxford University Press, ISBN 0198512880, New York

Murugaraj, P.; Mainwaring, D. & Mora-Huertas, N. (2005). Dielectric enhancement in polymer-nanoparticle composites through interphase polarizability. *J. Appl. Phys.,* 98, 054304/1-054304/6, ISSN 0021-8979

Murugaraj, P.; Mainwaring, D. & Mora-Huertas, N. (2006a). Thermistor behaviour in a semiconducting polymer-nanoparticle composite film. *J. Phys. D: Appl. Phys.*, 39, 2072-2078, ISSN 0022-3727

Murugaraj, P.; Mainwaring, D.E.; Jakubov, T.; Mora-Huertas, N.; Khelil, N.A. & Siegele, R. (2006b). Electron transport in semiconducting nanoparticle and nanocluster carbon-polymer composites. *Solid State Commun.,* 137, 422-426, ISSN 0038-1098

Murugaraj, P.; Mora-Huertas, N.; Mainwaring, D.E.; Ding, Y.; Agrawal, S. (2008). Influence of thermal stresses on electron transport in carbon-polymer nanocomposite films. *Composites, Part A,* 39A, 308-313, ISSN 1359-835X

Murugaraj, P.; Mainwaring, D. & Siegele, R. (2009a). Electron transport properties of irradiated polyimide thin films in single track regime. *Appl. Phys. Lett.,* 94, 122101/1-122101/3, ISSN 0003-6951

Murugaraj, P.; Mainwaring, D.E. & Mora-Huertas, N. (2009b). Electromechanical response of semiconducting carbon-polyimide nanocomposite thin films. *Compos. Sci. Technol.*, 69, 2454-2459 ISSN 0266-3538

Murugaraj, P.; Mainwaring, D.E.; Chen, L.G.; Sawant, P.; Al Kobaisi, M. & Yek, W.M. (2010a). Interfacial aspects of adhesion in polymer nanocomposite thin-film devices. *J. Appl. Polym. Sci.,* 115, 1054-1061, ISSN 0021-8995

Murugaraj, P.; Mainwaring, D.; Khelil, N.A.; Peng, J.L; Siegele, R. & Sawant, P. (2010b). The improved electromechanical sensitivity of polymer thin films containing carbon clusters produced in situ by irradiation with metal ions. *Carbon*, 48, 4230-4237, ISSN 0008-6223

Nandi, M.; Conklin, J.A.; Salvati Jr. L. & Sen, A. (1990). Molecular level ceramic/polymer composites. 1. Synthesis of polymer-trapped oxide nanoclusters of chromium and iron. *Chem. Mater.*, 2, 772-776, ISSN 0897-4756

Nelson, J. K. & Fothergill, J. C. (2004). Internal charge behaviour of nanocomposites. *Nanotechnology*, 15, 586-595, ISSN 0957-4484

Neugebauer, C.A. & Webb, M.B. (1962). Electrical conduction mechanism in ultrathin, evaporated metal films. *J. Appl. Phys.,* 33, 74-82, ISSN 0021-8979

O'Connor, C. J.; Buisson, Y. S. L.; Banerjee, S. Li S.; Premchandran, R.; Baumgartner, T.; John, V. T.; McPherson, G. L.; Akkara, J. A. & Kaplan, D. L. (1997). Ferrite synthesis in microstructured media: Template effects and magnetic properties. *J. Appl. Phys.* 81, 4741-4743, ISSN 0021-8979

Park, S-J.; Lee, E-J. & Kwon S-H. (2007). Influence of surface treatment of polyimide film on adhesion enhancement between polyimide and metal films. *Bull Korean Chem. Soc.,* 28, 188-192, ISSN 0253-2964

Phillips, H.M.; Wahi S. & Sauerbrey, R. (1993). Submicron electrically conducting wires produced in polyimide by ultraviolet laser irradiation. *Appl. Phys. Lett.* 62, 2572-2524, ISSN 0003-6951

Ranucci, E.; Sandgren, A.; Andronova, N. & Albertsson, A-C. (2001). Improved polyimide/ metal adhesion by chemical modification approaches. *J. Appl, Polym, Sci,.* 82, 1971-1985, ISSN 0021-8995

Rao, Y. & Wong, C.P. (2002). Novel ultra-high dielectric constant polymer based composite development for embedded capacitor application. *Proc. IEEE Electronic Packag. Technol. Conf.* 2002, 65-69, ISBN 0780374355, 10-12 December 2002, Singapore, IEEE Inc., Piscataway, USA

Rao, Y.; Ogitani, S.; Kohl, P. & Wong, C. P. (2002). Novel polymer–ceramic nanocomposite based on high dielectric constant epoxy formula for embedded capacitor application. *J. Appl. Polym. Sci.,* 83, 1084-1090, ISSN 0021-8995

Rao, Y. & Wong, C. P. (2004). Material characterization of a high-dielectric-constant polymer–ceramic composite for embedded capacitor for RF applications. *J. Appl. Polym. Sci.,* 92, 2228-2231, ISSN 0021-8995

Ree, M.; Chen, K-J.; Kirby, D. P.; Katzenellenbogen, N. & Grischikowsky, D. (1992). Anisotropic properties of high - temperature polyimide thin films: Dielectric and thermal - expansion behaviors. *J. Appl. Phys.,* 72, 2014-2021, ISSN 0021-8979

Rousset, A.; Legros, R. & Lagrange, A. (1994). Recent progress in the fabrication of ceramic negative temperature coefficient thermistors. J. Eur. Ceram. Soc., 13, 185-195, ISSN 0955-2219

Salvetat, J-P; Costantini, J-M.; Brisard, F.& Zuppiroli, L. (1997). Onset and growth of conduction in polyimide kapton induced by swift heavy-ion irradiation. *Phys. Rev. B: Condens. Matter,* 55, 6238-6248, ISSN 0163-1829

Shekhar, S.; Prasad, V. & Subramanyam, S.V. (2006a). Anomalous Efros-Shklovskii variable range hopping conduction in composites of polymer and iron carbide nanoparticles embedded in carbon. *Phys. Lett. A.* 360, 390-393, ISSN 0375-9601

Shekhar, S.; Prasad, V. and Subramanyam, S.V. (2006b). Structural and electrical properties of composites of polymer–iron carbide nanoparticles embedded in carbon. *Mater. Sci. Eng. B*, 133, 108–112, ISSN 0921-5107

Sheng, P.; Sichel, E.K. & Gittleman, J.L. (1978). Fluctuation induced tunnelling conduction in carbon-polyvinylchloride composites. *Phys. Rev. Letts.* 40, 1197-1200, ISSN 0031-9007

Sheng, P. (1980). Fluctuation-induced tunneling conduction in disordered materials. *Phy. Rev. B: Condens. Mater.,* 21, 2180-2195, ISSN 0163-1829

Sheng, P. & Klafter, J. (1983). Hopping conductivity in granular disordered systems. *Phy. Rev. B: Condens. Mater.,* 27, 2583-2586, ISSN 1094-1622

Sherman, R.D.; Middleman, L.M. & Jacobs, S.M. (1983). Electron transport processes in conductor-filled polymers. *Polym. Eng. Sci.,* 23, 37-47, ISSN 0032-3888

Shi, N & Ramprasad, R. (2007). Dielectric properties of nanoscale multi-component systems: A first principles computational study. *J. Comput.-Aided Mater. Des.,* 14, 133-139, ISSN 0928-1045

Shi, N & Ramprasad, R. (2008). Local properties at interfaces in nanodielectrics: An *ab initio* computational study. *IEEE Trans. Dielectr. Electr. Insul.,* 15, 170-177, ISSN 1090-9878

Srivastava, S.K.; Avasthi, D.K. & Pippel, E. (2006). Swift heavy ion induced formation of nanocolumns of C clusters in a Si based polymer. *Nanotechnology,* 17, 2518-2522, ISSN 0957-4484

Suzuki. S.; Bower, C.; Kiyokura, T.; Nath, K.G.; Watanabe,Y. & Zhou, O. (2001). Photoemission spectroscopy of single walled carbon nanotube bundles. *J. Electron. Spectrosc. Relat. Phenom.,* 114–116, 225–228, ISSN 0368-2048

Thermometrics, www.thermometrics.com/assets/imges/ntcnotes.pdf

Todd M. G. & Shi, F. G. (2003). Characterizing the interphase dielectric constant of polymer composite materials: Effect of chemical coupling agents. *J. Appl. Phys.,* 94, 4551-4557, ISSN 0021-8979

Toulemonde, M.; Trautmann, C.; Balanzat, E.; Hjort, K. & Weidinger, A. (2004). Track formation and fabrication of nanostructures with MeV-ion beams. *Nucl. Instrum. Methods Phys. Res. Sect. B*, 216, 1-8, ISSN 0168-583X

Trung, T.; Trung, T.H. & Hab, C-S. (2005). Preparation and cyclic voltammetry studies on nickel-nanoclusters containing polyaniline composites having layer-by-layer structures. *Electrochim. Acta,* 51, 984–990, ISSN 0013-4686

Ulrich, R. (2004). Matching embedded capacitor dielectrics to applications. *Circuit World*, 30, 20-24, ISSN 0305-6120 and references therein

Van Zyl, W. E.; Garcia, M.; Schruwen, B. A. G.; Kooi, B. J.; Hosson, J. T. M. & Verweij, H. (2002). Hybrid polyamide/silica nanocomposites: synthesis and mechanical testing. *Macromol. Mater. Eng.,* 287, 106-110, ISSN 1438-7492

Vo, H.T. & Shi, F. G. (2002). Towards model-based engineering of optoelectronic packaging materials: dielectric constant modeling. *Microelectron. J.,* 33, 409-415, ISSN 0026-2692 and references therein

Wei, H. & Eilers, H. (2008). Electrical conductivity of thin-film composites containing silver nanoparticles embedded in a dielectric fluoropolymer matrix. *Thin Solid Films,* 517, 575–581, ISSN 0040-6090

Zhang, R.; Baxendale, M. & Peijs, T. (2007). Universal resistivity-strain dependence of carbon nanotube/polymer composites. *Phys. Rev. B: Condens. Matter Mater. Phys.,* 76, 195433/1-195433/5, ISSN 1098-0121

Ziegler, J.F.; Biersack, J.P. & Ziegler, M.D. (2008) http://www.srim.org/ SRIM - SRIM Co.. ISBN 0-9654207-1-X

Zhu, D.; Bin, Y. & Matsuo, M. (2007) Electrical conducting behaviors in polymeric composites with carbonaceous fllers. *Journal of Polym. Sci. Part B*: Polym. Phys., 45, 1037–1044, ISSN 0887-6266
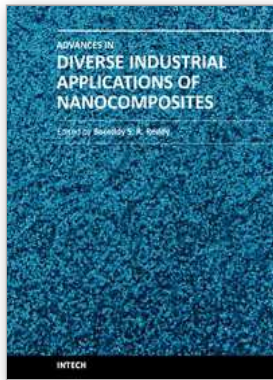
Advances in Diverse Industrial Applications of Nanocomposites
Edited by Dr. Boreddy Reddy

Nanocomposites are attractive to researchers both from practical and theoretical point of view because of combination of special properties. Many efforts have been made in the last two decades using novel nanotechnology and nanoscience knowledge in order to get nanomaterials with determined functionality. This book focuses on polymer nanocomposites and their possible divergent applications. There has been enormous interest in the commercialization of nanocomposites for a variety of applications, and a number of these applications can already be found in industry. This book comprehensively deals with the divergent applications of nanocomposites comprising of 22 chapters.

How to reference
In order to correctly reference this scholarly work, feel free to copy and paste the following:

Pandiyan Murugaraj and David Mainwaring (2011). Electronic Functionality of Nanocomposites, Advances in Diverse Industrial Applications of Nanocomposites, Dr. Boreddy Reddy (Ed.), ISBN: 978-953-307-202-9, InTech, Available from: http://www.intechopen.com/books/advances-in-diverse-industrial-applications-of-nanocomposites/electronic-functionality-of-nanocomposites

INTECH
open science | open minds